

Modeling complex aquifer systems: a case study in Baton Rouge, Louisiana (USA)

Hai V. Pham¹ · Frank T.-C. Tsai²

Received: 4 May 2016 / Accepted: 29 December 2016 / Published online: 21 January 2017
© Springer-Verlag Berlin Heidelberg 2017

Abstract This study targets two challenges in groundwater model development: grid generation and model calibration for aquifer systems that are fluvial in origin. Realistic hydrostratigraphy can be developed using a large quantity of well log data to capture the complexity of an aquifer system. However, generating valid groundwater model grids to be consistent with the complex hydrostratigraphy is non-trivial. Model calibration can also become intractable for groundwater models that intend to match the complex hydrostratigraphy. This study uses the Baton Rouge aquifer system, Louisiana (USA), to illustrate a technical need to cope with grid generation and model calibration issues. A grid generation technique is introduced based on indicator kriging to interpolate 583 wireline well logs in the Baton Rouge area to derive a hydrostratigraphic architecture with fine vertical discretization. Then, an upscaling procedure is developed to determine a groundwater model structure with 162 layers that captures facies geometry in the hydrostratigraphic architecture. To handle model calibration for such a large model, this study utilizes a derivative-free optimization method in parallel computing to complete parameter estimation in a few months. The constructed hydrostratigraphy indicates the Baton Rouge aquifer system is fluvial in origin. The calibration result

indicates hydraulic conductivity for Miocene sands is higher than that for Pliocene to Holocene sands and indicates the Baton Rouge fault and the Denham Springs-Scotlandville fault to be low-permeability leaky aquifers. The modeling result shows significantly low groundwater level in the “2,000-foot” sand due to heavy pumping, indicating potential groundwater upward flow from the “2,400-foot” sand.

Keywords Conceptual models · Groundwater system · Hydrostratigraphy · Geostatistics · USA

Introduction

Numerical models have been widely used in recent decades to study groundwater flow in subsurface systems. However, developing groundwater models has never been an easy task for fluvial-in-origin subsurface systems owing to their inherent structural heterogeneity (Galloway 1977). The first challenge in developing a groundwater model is to adequately characterize the subsurface systems. The literature shows many methods to model hydrofacies for different heterogeneity scales using various input data sets (e.g., well logs, pumping test, and seismic data). Among them, widely used methods in hydrogeology are the two-point variogram statistics, such as indicator geostatistics (Journel 1983; Johnson and Dreiss 1989; Johnson 1995; Proce et al. 2004); transition probability-based indicator geostatistics (Carle and Fogg 1996; Lee et al. 2007; Koch et al. 2014); and multiple-point simulation (MPS) (Strebelle 2002; Journel 2005; dell’Arciprete et al. 2012). Reviews of these methods can be found in Koltermann and Gorelick (1996), de Marsily et al. (2005), and Hu and Chugunova (2008). While the applications of these methods are site specific and are subject to user preference and expertise, it has been well understood that

✉ Frank T.-C. Tsai
ftsai@lsu.edu

Hai V. Pham
hpham28@lsu.edu

¹ Department of Civil and Environmental Engineering, Louisiana State University, 3526D Patrick F. Taylor Hall, Baton Rouge, LA 70803, USA

² Department of Civil and Environmental Engineering, Louisiana State University, 3526B Patrick F. Taylor Hall, Baton Rouge, LA 70803, USA

different hydrofacies methods generate significantly different spatial distributions of hydraulic properties (Alabert and Modot 1993; Gómez-Hernández and Wen 1998; Western et al. 2001; Zinn and Harvey 2003; Zhang et al. 2006; Lee et al. 2007; Bianchi et al. 2011; Berg and Illman 2015) and consequent flow and solute transport responses.

The second challenge in developing a groundwater model, besides the estimation of spatially variable hydraulic parameters, is to construct better model grids that are consistent with the geometries of modelled hydrofacies. Errors from inaccurate model grids that fail to capture hydrofacies geometries may result in incorrect estimated hydraulic parameters during model calibration. The literature shows two approaches commonly used to construct a computational grid from well log data: the solid approach and the pre-defined grid approach. Before implementing either approach, one needs to obtain geological information (e.g., lithology, bed boundary elevation, formation dip, etc.) from well logs. Readers are referred to some classic books for well log interpretation techniques (Schlumberger 1972; Hilchie 1982; Bassiouni 1994), which were used to interpret well logs for this study.

Using the solid approach, one needs to manually correlate well logs and label distinct hydrofacies for each well log. Once the well log correlation is established, interpolation methods are applied to generating surfaces of the same types of hydrofacies. These surfaces represent the hydrofacies boundaries and result in a solid model. Jones et al. (2002) and Lemon and Jones (2003) developed a grid generator to generate computational grids for groundwater models from solid models. The beauty of this approach is the creation of non-uniform computational layers that match well the generated hydrofacies surfaces, including pinch-outs.

The biggest challenge in using this approach is performing manual correlation between well logs, which is subjective and can become laborious and impractical when dealing with a huge number of well logs in areas known to be highly complex. (e.g., fluvial depositional environments). Manually correlating well logs often results in inconsistencies with geological deposition, forces correlation of unrelated hydrofacies, and produces erroneous hydraulic connections of discontinuous hydrofacies.

The pre-defined grid approach usually generates uniform, relatively coarse layers directly to be used for flow and transport modeling. Examples of this approach include using T-PROGS (Carle 1999) and geostatistical tools—e.g., GSLIB (Deutsch and Journel 1997). This approach does not force generating surfaces of hydrofacies, and therefore, avoids the issues caused by manual correlation; however, the greatest concern of using pre-defined grids is to lose the vertical resolution of hydrofacies geometries if layers are not fine enough. Using very fine layers intuitively can improve vertical resolution of hydrofacies geometry, but will significantly increase

computation time since pre-defined grids are directly used for flow simulation.

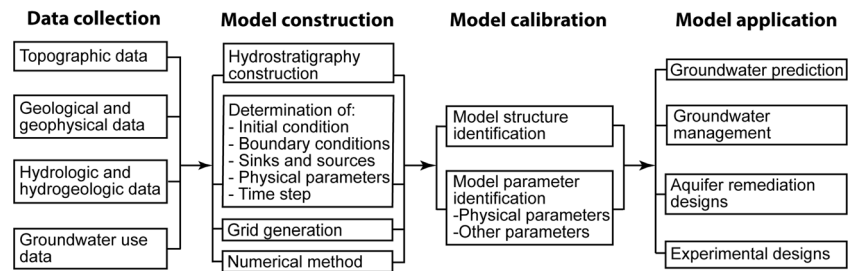
The third challenge when developing a groundwater model is model calibration; for complex aquifer systems, model calibration can be very time consuming. Without advanced search algorithms and computing resources, searching for better parameter values can end prematurely; moreover, grid error amplifies parameter estimation error. Model calibration may result in over-parameterization and unrealistic model parameter values in order to compensate model structure error due to an invalid grid.

This study presents a general procedure to develop complex groundwater models for siliciclastic aquifer systems and to overcome the challenges raised by grid generation and model calibration. The study first introduces a grid generation technique that maintains high vertical resolution of hydrofacies geometries with a reasonable number of non-uniform boundary-fitted layers. Second, the study adopts the covariance matrix adaptation-evolution strategy (CMA-ES; Hansen and Ostermeier 2001; Hansen et al. 2003) in parallel computing to calibrate complex groundwater models. Third, the grid generation and model calibration techniques are applied to developing a three-dimensional (3D) groundwater model for the fluvial-in-origin aquifer system underneath the Baton Rouge area, southeastern Louisiana.

Methodology

The flowchart in Fig. 1 presents major steps to develop a groundwater model for applications: data collection, model construction, model calibration, and model application. The first step is to collect and analyze pertinent data for the area of interest. The data include geological and geophysical data as well as hydrologic and hydrogeologic data, groundwater use data, etc. Data are always lacking for groundwater study and their quantity and quality directly affect the subsequent model development steps. The second step is to construct a conceptual groundwater model based on the collected data. Modelers often face decisions of which model components are fixed and which model components are to be adjusted in the model calibration phase. In model construction, hydrostratigraphy is the backbone of a groundwater model and directly controls the development of a computational grid for a numerical method. Hydrostratigraphy construction for an aquifer system is the key step to transfer known geological information from well logs to a groundwater model. This step is actually extremely difficult for a complex aquifer system such as the siliciclastic groundwater system in this study, but is often overlooked and overly simplified. The challenge leads to this study to address the question of how to use a large amount of well logs with highly irregular sand-clay sequences to generate a proper computational grid for groundwater modeling.

Fig. 1 Flow chart for developing a groundwater model



Model calibration is a necessary step to ensure model integrity before a groundwater model can be applied to its applications. It involves tuning physical parameters (e.g., hydraulic conductivity, specific storage, etc.) and adjusting model components such that groundwater model output is close to observed data. For complex aquifer systems, model calibration can be time consuming.

This section focuses on two challenges in groundwater model development: grid generation and model calibration. The discussions in the following are mainly for siliciclastic sedimentary depositional environments, which are applicable to this case study demonstration.

Well log interpretation

The primary sources of information used to establish hydrofacies geometries are wire-line spontaneous potential (SP) and electrical resistivity logs for boreholes. Spontaneous potential and resistivity log responses are controlled largely by the ratio of sand to clay minerals and they have long been used to interpret sedimentary depositional environments. Galloway (1977) used SP and resistivity curve morphologies to identify fluvial facies for channel fill, levee, crevasse splay and floodplain, and established a meandering stream facies. Kerr and Jirik (1990) adapted Galloway’s (1977) facies model and provided examples of SP and resistivity responses that match known fluvial facies for the middle Frio formation, South Texas. Sands deposited by braided streams produce jagged, wedge-shaped curve morphologies (Miall 2010). Based on these established relationships between log responses and fluvial facies, Chamberlain et al. (2013) used SP and resistivity data to study depositional environments of siliciclastic sediments in the Baton Rouge area.

Following Chamberlain et al. (2013) and Elshall et al. (2013), this study uses SP, resistivity, and gamma ray (when available) to identify the location of sand facies at depth. Figure 2 shows a typical SP-resistivity log for saturated formations in the Baton Rouge area. Based on deviations from a visually estimated shale baseline, boundaries of sands can be drawn on inflection points of SP curves. A cutoff value that generally fell between 10 and 35 ohm-m for resistivity curves is assigned to determine boundaries of sands. Low long-

normal resistivity generally indicates the occurrence of salty water. Low gamma ray response generally indicates a sand facies. Sand boundaries can be well identified by correlating SP, resistivity and gamma ray curves (Schlumberger 1972;

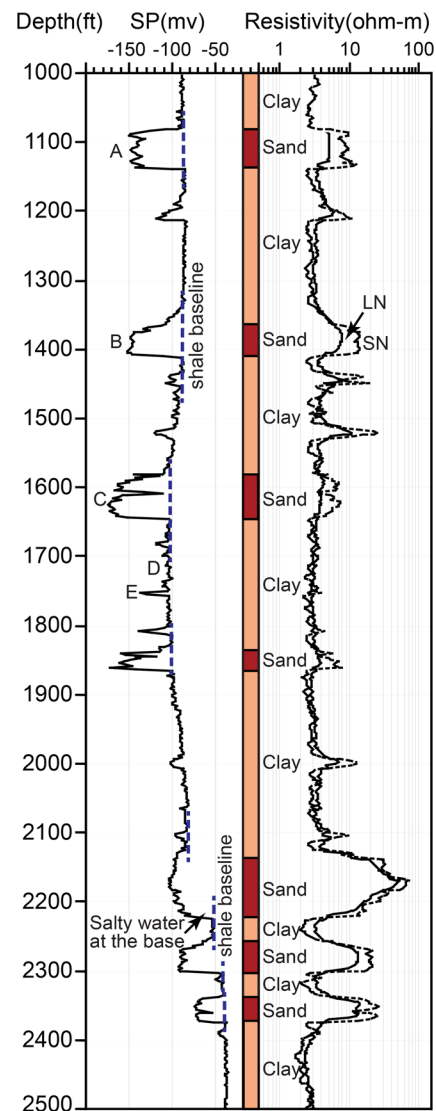


Fig. 2 Interpretation of fluvial facies for a well log. Legend: A amalgamated braided channel-fill with brackish water, B channel-fill point bar sand with brackish water, C stacked/amalgamated channel-fill with very salty water, D floodplain, and E natural levee (Kerr and Jirik 1990; Miall 2010). SN short normal resistivity (dashed line); LN long normal resistivity (solid line). 1,000 ft = 304.8 m

Hilchie 1982; Bassiouni 1994)—for example, seven sand facies are picked and many thin sands are ignored as shown in Fig. 2. Non-sand intervals are assumed to be clay (shale or mudstone) facies.

Well log interpretation is inevitably subjected to an individual's experience and the purpose of the work. This study does not intend to discuss the uncertainty of computational grids due to different log interpretations. Moreover, it is possible to use the established relationships between log responses and fluvial facies from Galloway (1977), Kerr and Jirik (1990), and Miall (2010) to infer different fluvial facies—for example, Fig. 2 shows some identified fluvial facies based on the established relationships. This study does not intend to identify specific fluvial facies, but focuses on aquifer system construction using identified sand and clay facies from well logs.

Indicator kriging for hydrostratigraphy construction

To construct hydrostratigraphy based on the aforementioned well log interpretation of sand-clay sequences, well logs are first transformed into binary indicator values. The indicator value for sand facies is 1 and for clay facies is 0. The indicator kriging (Johnson and Dreiss 1989) is suitable for handling bimodal heterogeneity. By using a regional geological dip to correlate well logs as shown in Fig. 3a, indicator kriging is performed on inclined surfaces where indicator data are obtained at the intersections with well logs. To make it easier for operating indicator kriging, all well logs are translated vertically to a non-dipping domain. To do so, the vertical translation distance depends on the dip angle and the distance from well log location to a strike line that serves as a pivot as illustrated in Fig. 3b. Then, indicator kriging is performed on horizontal surfaces given horizontal discretization, which can be done by any methods available in the literature. The same horizontal discretization is applied to all horizontal surfaces at different depths. A detailed 3D hydrostratigraphic architecture can be achieved by assembling a large number of horizontal surfaces with fine intervals. This study conducts indicator kriging at horizontal surfaces with one-foot intervals.

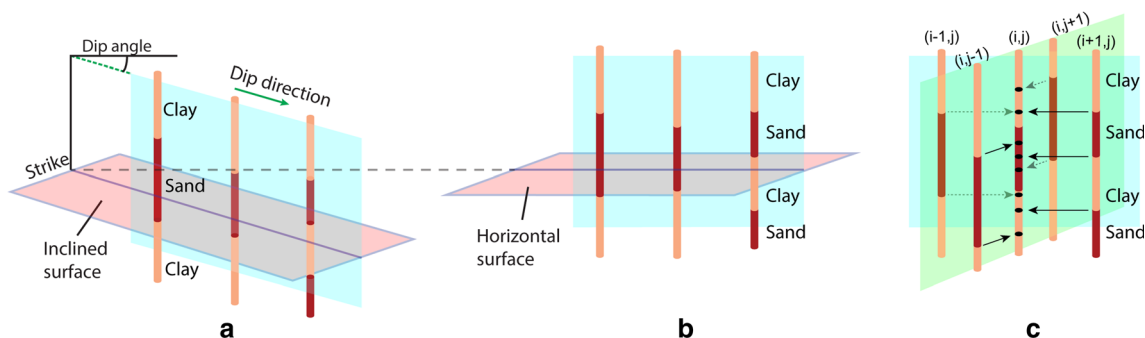


Fig. 3 Translation of well log positions from **a** a dipping surface to **b** a non-dipping surface. **c** An illustration of bed boundary projection for the vertical column (i, j) of a grid. Bed boundaries of neighboring vertical columns are projected to the vertical column (i, j)

Finally, the 3D hydrostratigraphic architecture is transformed to a dipped architecture that follows the dip direction.

It is noted that the grid generation technique in this study is not limited to indicator kriging. Any geostatistical method can be used to estimate hydrofacies for a surface. The resulting indicator data from horizontal surfaces are used to compute experimental variograms. Then, a variogram model can be derived by fitting to the experimental variograms.

The expected value of the indicator at an unobserved location is obtained by

$$v(\mathbf{x}_0) = \sum_{i=1}^S \lambda_i I(\mathbf{x}_i) \quad (1)$$

where $v(\mathbf{x}_0)$ is the expected value at unobserved location \mathbf{x}_0 , S is the number of well logs for a horizontal surface, and λ_i are the indicator kriging weights. Indicator kriging has been well documented in the literature. Readers are referred to Olea (1999) for more information.

The expected value of indicator function represents the probability that facies at a location \mathbf{x}_0 fall into sand facies or clay facies. By giving a cutoff α as follows, distributed sand and clay facies on a horizontal surface can be achieved:

$$I(\mathbf{x}_0) = \begin{cases} 1 & : \text{ sand if } v(\mathbf{x}_0) \geq \alpha \\ 0 & : \text{ clay if } v(\mathbf{x}_0) < \alpha \end{cases} \quad (2)$$

Determination of a defensible cutoff value is challenging. A value of 0.5 is commonly used for a neutral selection. However, a better cutoff can be determined in a calibration process where facies estimates are subject to additional information, e.g., driller's logs, total volume of sand or clay facies from electrical logs, etc. (Elshall et al. 2013).

Upscale hydrostratigraphic architecture to a model grid

The MODFLOW model (Harbaugh 2005) uses a structured grid where cells are rectangular in the two-dimensional plane. The 3D model domain is discretized into rows, columns, and layers, ordered in a Cartesian coordinate system. Each grid

cell (except for those at model boundaries) is connected to six surrounding cells. Unlike the unstructured grid version of MODFLOW-USG (Panday et al. 2013) that has more flexibility for domain discretization, the challenge for conventional MODFLOW models is that all computational layers in the structured grid must be continuous throughout the model domain. Once a hydrostratigraphic architecture with very fine vertical discretization is generated by indicator kriging, the following two steps are developed to upscale the hydrostratigraphic architecture to a MODFLOW structured grid by merging the same hydrofacies in the vertical direction to reduce the number of layers.

Step 1. Project neighboring bed boundaries. To account for the continuity of MODFLOW layers throughout the model domain, Fig. 3c illustrates bed boundary projection for each vertical column of a grid. A vertical column (i, j) of a grid in Fig. 3c originally has four bed boundaries and has direct connections to its neighboring vertical columns which have different bed boundary positions. The bed boundaries of the neighboring vertical columns are projected to the vertical column (i, j) and increase bed boundaries of the vertical column (i, j) to 12. Bed boundary projection is applied to all vertical columns of the grid. By doing so, each vertical column of the grid possesses information of bed boundary positions of its neighboring vertical columns. Bed boundary projection is an important step in order to preserve the continuity of flow pathways, especially through geological faults, pinch-out areas, or narrow connections.

Step 2. Determine model layers. Given a desired number of model layers, this study introduces a “ruler” algorithm to assign MODFLOW layer indices to each vertical column. Again, the layer boundaries are required to match the bed boundaries. As shown in Fig. 4a, the start and end of the ruler match the top and bottom boundaries of a vertical column, respectively. The number of major ticks in the ruler represents the number of MODFLOW layers. The number of layers up to a bed boundary for a vertical column is obtained by comparing its bed boundary location to the ruler—for example, a bed boundary located between 0 and 1.5 in the ruler indicates one layer up to the bed boundary, between 1.5 and 2.5 indicates two layers up to the bed boundary, between 2.5 and 3.5 indicates three layers up to the bed boundary, and so forth. When the thickness between consecutive bed boundaries is small, the ruler algorithm is likely to assign two or more bed boundaries with the same number of layers up to their bed boundaries as shown in Fig. 4b. In this case, the ruler

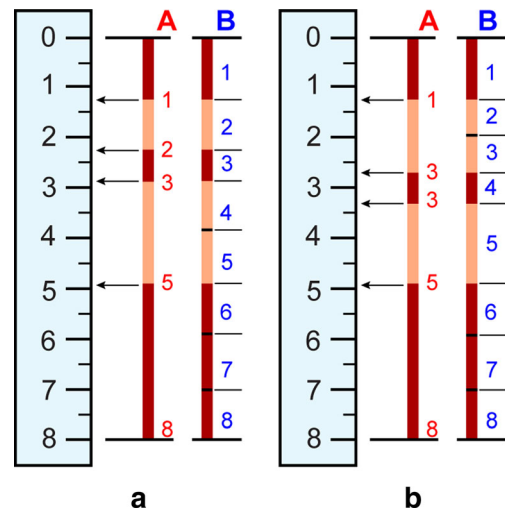


Fig. 4 Illustration of the ruler algorithm: **a** a vertical column of a grid with a distinct number of layers up to each bed boundary, and **b** a vertical column of a grid with two bed boundaries having the same number of layers. *A* refers to the number of layers up to a bed boundary and *B* model layer indices

algorithm will adjust the numbers to make sure that each bed boundary has a distinct layer index. In the last step, equal thickness of layers is given to segments that need to be divided into two or more layers based on the final assignment of the layer indices to the bed boundaries.

Model calibration using parallel computing

Model calibration is the process of adjusting model parameter values until a satisfactory fit between model outputs and field measurements (e.g., heads, concentrations) is achieved. Traditionally, model calibration is performed manually based on trial-and-error methods. This approach is easy to apply, but is laborious and time-consuming; furthermore, trial-and-error methods may not guarantee finding the best solutions because different user’s manipulations may produce dissimilar solutions.

Automatic model calibration using optimization methods is efficient due to their ability to handle a high number of model parameters and the accuracy of solutions. Optimization methods can be classified as derivative-based and non-derivative-based search methods (global search methods). Derivative-based methods converge quickly, but solutions may be trapped to local optima. Global search methods have potential to find near global solutions as well as handling non-differentiable and discontinuous functions. Popular global search methods applied to groundwater model calibration include

genetic algorithms (El Harrouni et al. 1996; Wang 1997; Karpouzou et al. 2001), simulated annealing and tabu search (Zheng and Wang 1996), ant colony optimization (Abbaspour et al. 2001), particle swarm (Gill et al. 2006; Krauß and Cullmann 2012), and shuffled complex evolution (SCE) (Vrugt et al. 2003). The common disadvantage of global search methods is that a large number of model runs and iterations are needed in order to reach a near global solution. For a computationally expensive simulation model, this method may become impractical; this problem, however, can be solved efficiently by parallel computing. Reviews and comparisons of methods for model calibration can be found in many books and articles (Cooley 1985; Sun 1994; Hunt et al. 2007; Hill and Tiedeman 2007; Vrugt et al. 2008; Hendricks Franssen et al. 2009; Fienen et al. 2009; Doherty 2015; Yeh 2015). Popular software for automatic groundwater model parameter estimation include PEST (Doherty et al. 1994), UCODE (Poeter and Hill 1999), or MGO (Zheng and Wang 2003).

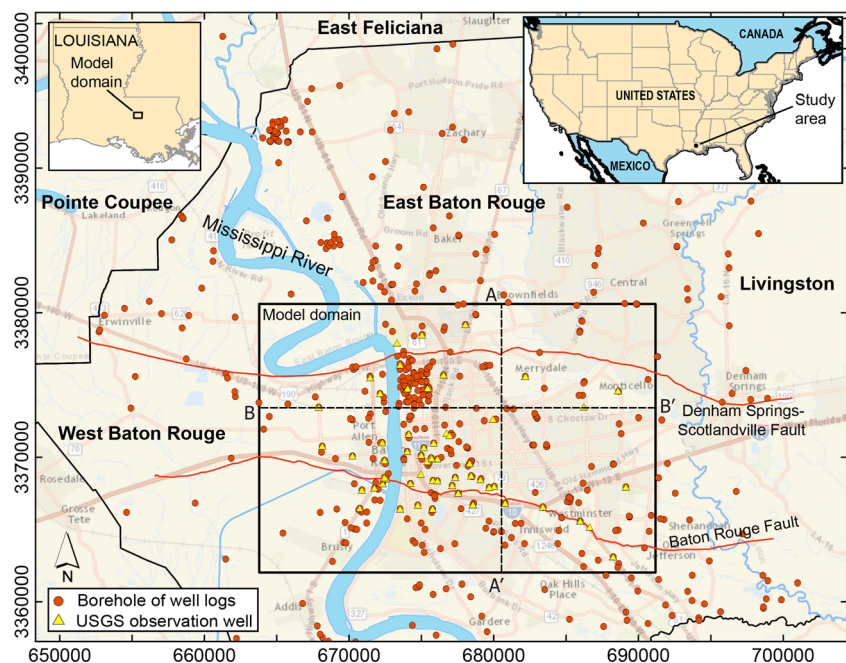
This study adopts CMA-ES (Hansen and Ostermeier 2001; Hansen et al. 2003) as a global search method to calibrate a groundwater model and estimate model parameters for three key reasons. First, CMA-ES has the capability of obtaining a near global solution and avoiding entrapment in local optima. Second, CMA-ES provides a full covariance matrix of estimated parameters, which can be used to assess parameter estimation and prediction uncertainty. Third, CMA-ES can be implemented in a high-performance computing system to overcome the prohibitive computational cost (Elshall et al. 2015).

Construction of Baton Rouge aquifer system, southeastern Louisiana

The Baton Rouge aquifer system shown in Fig. 5 is part of the Southern Hills regional aquifer system, southeastern Louisiana, USA. The Baton Rouge aquifer system consists of a succession of south-dipping siliciclastic sandy units and mudstones of Miocene through Holocene age, extended to a depth of 3,000 ft (914 m; Meyer and Turcan 1955), and is highly complex as a result of fluvial deposition (Chamberlain et al. 2013). Eleven freshwater aquifers underneath Baton Rouge are the Mississippi River Alluvial Aquifer (MRAA), the “400-foot” sand, the “600-foot” sand, the “800-foot” sand, the “1,000-foot” sand, the “1,200-foot” sand, the “1,500-foot” sand, the “1,700-foot” sand, the “2,000-foot” sand, the “2,400-foot” sand, and the “2,800-foot” sand. These aquifers were named by their approximate depth below ground level in the Baton Rouge Industrial District (Meyer and Turcan 1955). The depth of the MRAA in the model domain is similar to the “400-foot” sand. The sand deposition is non-uniform due to spatial and temporal variations in fluvial processes as well as a large amount of missing sand possibly due to erosional unconformity. From the region-scale study of Griffith (2003), the Baton Rouge aquifer system dips south towards the Gulf of Mexico.

The Baton Rouge aquifer system consists of the east–west trending Baton Rouge fault and the Denham Springs–Scotlandville fault. The faults crosscut the aquifer/aquitard sequence in the study area (McCulloh and Heinrich 2013). The Denham Springs–Scotlandville fault is generally thought to have no significant effect on groundwater flow. The

Fig. 5 Map of the study area, boreholes of well logs (circles), and US Geological Survey groundwater observation wells (triangles). The coordinate system is UTM (meters), Zone 15, NAD83



historical groundwater data suggests the Baton Rouge fault to be a horizontal flow barrier that separates the freshwater to the north and the saline water to the south. The source of saline water is likely from the expulsion of over-pressured brine fluids, extending vertically upward above the top of Gabriel salt dome all the way to the water table (Anderson et al. 2013). Bense and Person (2006) suggested the Baton Rouge fault to be a conduit-barrier fault. Recent study (Elshall et al. 2015) suggested the Baton Rouge fault and the Denham Springs-Scotlandville fault to be low-permeability leaky faults.

Groundwater naturally flows southward; however, excessive groundwater withdrawals in the area between two faults have caused significant declines of groundwater levels north of the Baton Rouge fault. The two largest pumping areas that cause the most significant drawdown are the Industrial District and the Lula pump station. The pumping wells at the Industrial District were screened from the “400-foot” sand to the “2,000-foot” sand. The “2,000-foot” sand is the most heavily pumped by the industrial wells. The Lula pump station heavily pumps the “1,500-foot” sand for public supply. The declines of groundwater level caused land subsidence (Whiteman 1980) and reversed the flow direction in the vicinity of the Baton Rouge fault to cause saltwater intrusion (Morgan and Winner 1964; Whiteman 1979; Tomaszewski 1996). Observed chloride concentrations are generally much less than a few thousand mg/L (Lovelace 2007). To better understand the impacts of the geological faults and the groundwater withdrawals on groundwater level decline, this study applied the proposed methodology to develop a Baton Rouge groundwater model, which covers the 11 sands.

Saltwater intrusion modeling and subsidence modeling were not conducted in this study. To the best of authors’ knowledge, the extent of subsidence does not affect groundwater flow in the Baton Rouge area. However, potential simulation errors in groundwater levels may occur near or in the south of the Baton Rouge fault where high chloride concentrations are present. Since this study used the developed groundwater model to investigate groundwater budget and flow patterns, the errors due to the density effect would not be significant. Nevertheless, saltwater intrusion modeling and subsidence modeling are important to the Baton Rouge area and will be the focus of future studies.

Results and discussion

Well log interpretation and hydrostratigraphic architecture

Using the method in sections ‘Well log interpretation’ and ‘Indicator kriging for hydrostratigraphy construction’, the study analyzed wireline well logs from 583 boreholes (Fig. 5). The result of binary well log interpretation is shown

in Fig. 6a. The number of sand and clay segments in well logs ranges from 3 to 59. It is impractical to manually build correlations between boreholes. The model domain in the planar direction is discretized into 93 rows and 137 columns with a cell size 200×200 m, resulting in 12,741 grid cells. Indicator kriging was adopted to construct a hydrostratigraphic architecture with a dip angle 0.29° and a cutoff value 0.40 from a prior study (Elshall et al. 2013). After translating all well logs vertically to a non-dipping domain, indicator kriging was conducted on horizontal surfaces of 1 ft (0.304 m) intervals from land surface to –2,890 ft (–881 m) below NGVD29 that covers the 11 sands. This study adopted an isotropic exponential variogram model (nugget = 0.084, range = 8,600 m, and sill = 0.223) for the indicator kriging (see Fig. 6b). The modeling area was divided into three regions by two fault lines. Hydrostratigraphic architecture for each region was constructed by the indicator kriging; then, the three hydrostratigraphic architectures were put together as shown in Fig. 6b. The presence of a large number of small facies thickness indicates a fluvial deposition environment, involving a wide mixture of grain sizes (e.g., from gravel to clay), a broad range of grain-size sorting (e.g., from poorly sorted to nearly homogeneous facies), and a wide-ranging interconnectivity between lithostratigraphic facies (e.g., at scales ranging from tens of meters to centimeters; Bowling et al. 2005). Figure 6b reveals the complexity of the Baton Rouge aquifer system, such as unconformity of sand units, interbedded clays, isolated sands, coalescences, and pinch-outs.

Moreover, facies displacement at the faults and hydraulic connection across the faults can also be identified. It was found for deeper sands that the vertical offset of the Baton Rouge fault is about 80 m at the “1,200-foot” sand and about 100 m at the “2,000-foot” sand. The vertical offset of the Denham Springs-Scotlandville fault at the “1,200-foot” sand is about 35 m and at the “2,000-foot” sand is about 70 m (Elshall et al. 2013). The offsets increase with depth. Figure 7 presents the architectures of the Baton Rouge fault and the Denham Springs-Scotlandville fault. White areas show potential hydraulic connections formed by juxtaposition of sand units at the faults. The figure indicates complex sand deposition and erosion through the fluvial process and the faulting process.

Model grid

It is obvious that a highly complex 3D MODFLOW grid is necessary in order to represent the Baton Rouge aquifer system. Using the proposed method in section 2.3, a grid of 162 model layers was constructed by upscaling the hydrostratigraphy. There are 808,078 active computational cells shown in Fig. 8. The model grid accurately matches the hydrostratigraphic architecture (Fig. 6a) and preserves layer

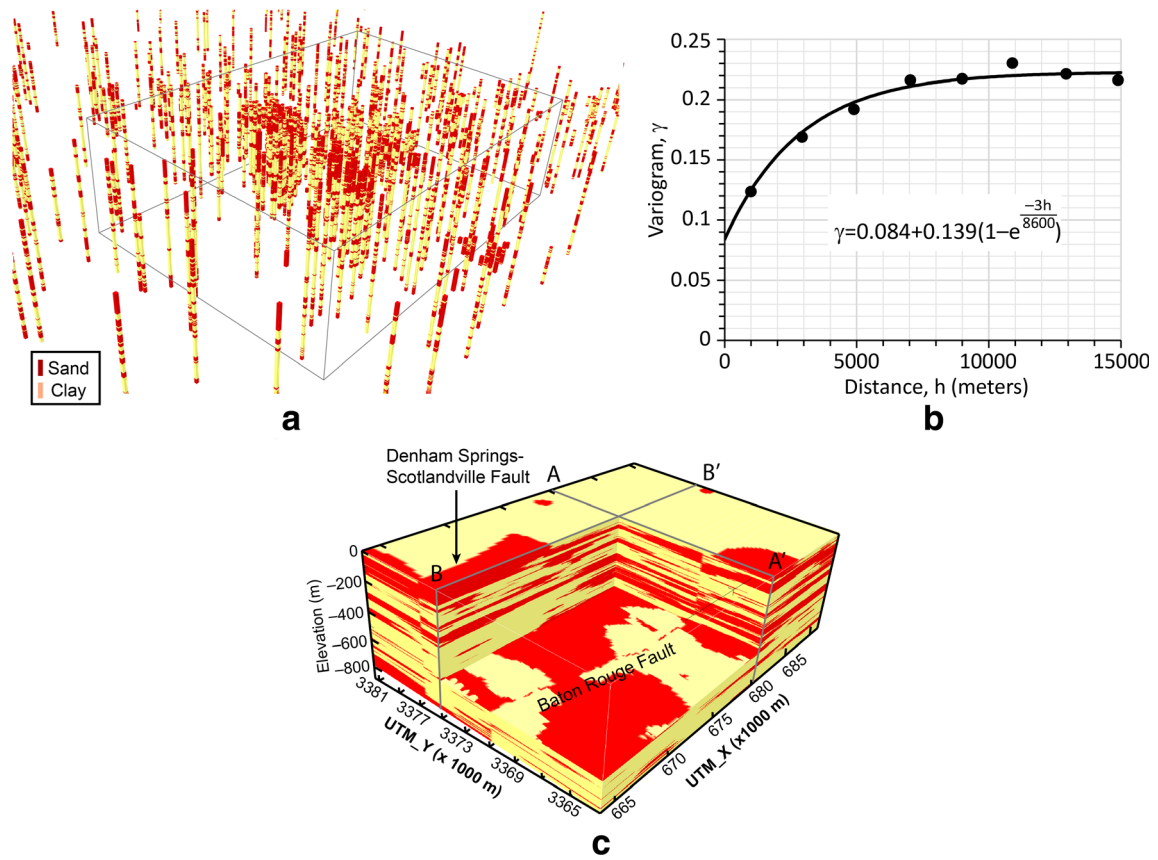


Fig. 6 Construction of hydrostratigraphic architecture from well logs: **a** distribution of sand and clay segments in boreholes as the result of well log interpretation, **b** exponential indicator variogram model. *Black dots*

are experimental indicator variograms, and **c** hydrostratigraphic architecture. The vertical exaggeration is 10

continuity. Each cell is 200 × 200 m with the cell thickness ranging from 3.05 to 30.5 m. The average thickness of the layers is 5.2 m. With this grid generation technique, the pumping wells are correctly positioned in their corresponding sands. Updating the model grid is straightforward when new well logs become available.

Groundwater model conceptualization

Using the generated MODFLOW grid, this section develops a groundwater model for the Baton Rouge area. The conceptual model structure is based on Fig. 8. The simulation period is from January 1, 1975 to December 31, 2014. The historical

Fig. 7 The architecture of **a** the Denham Springs-Scotlandville fault and **b** the Baton Rouge fault. *Red and cyan areas* indicate clay facies at the north and the south of each fault, respectively. *White areas* are potential hydraulic connections. The faults lines in the model domain are shown in Fig. 5

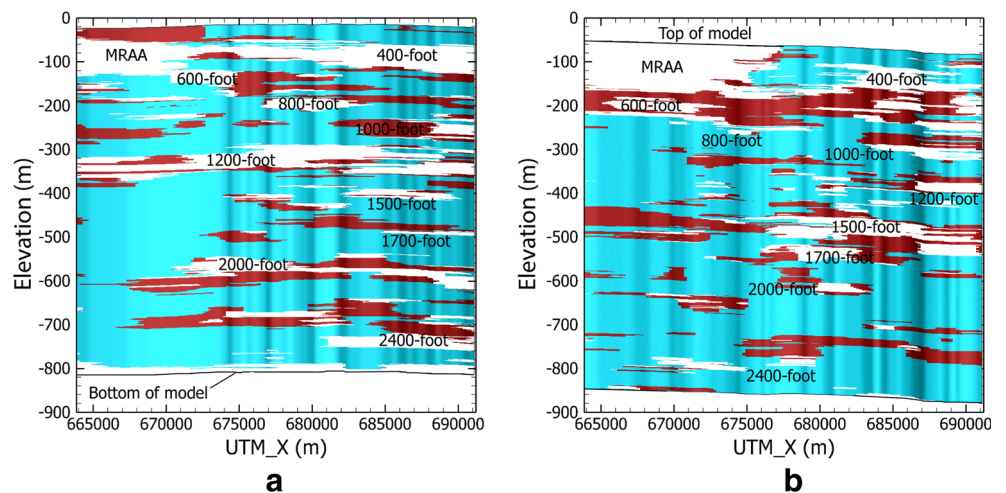
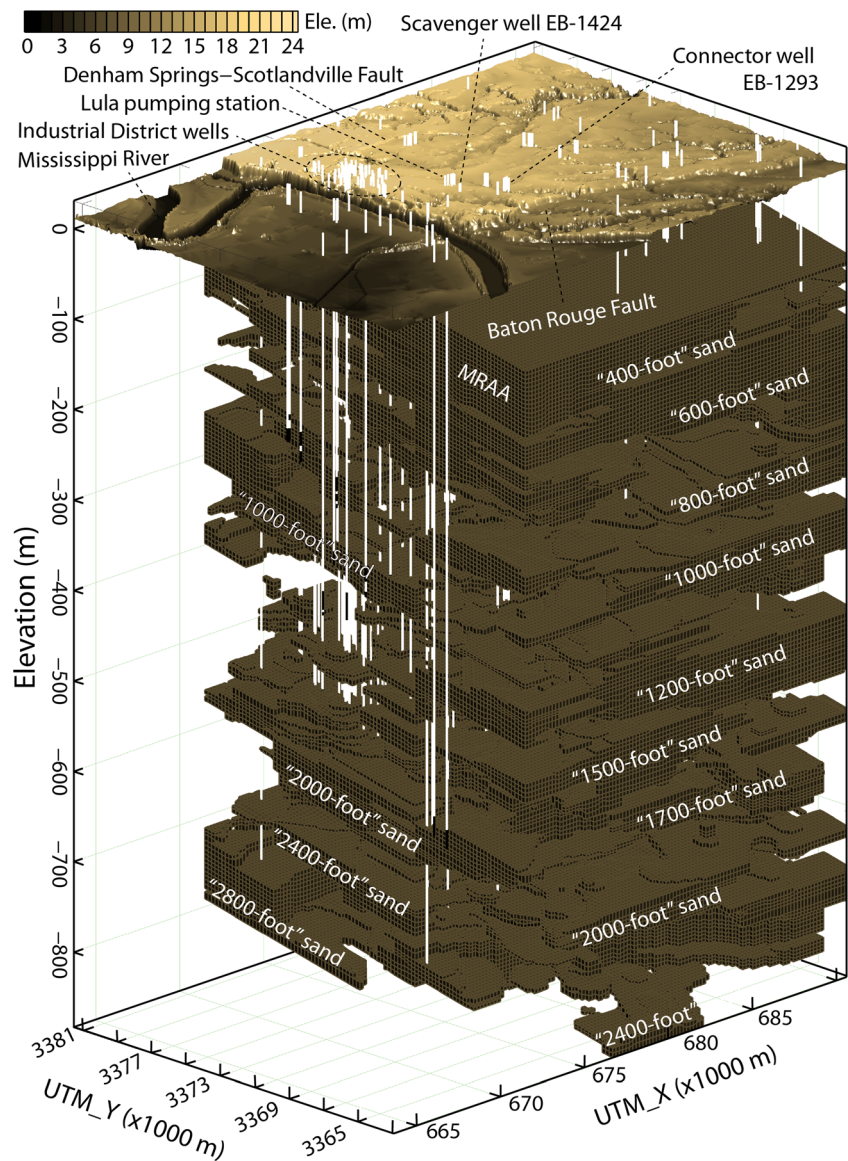


Fig. 8 Conceptual groundwater model for the Baton Rouge aquifer system, including 11 aquifers, two geological faults, and pumping and injection wells



groundwater head data in the simulation period were collected from 42 US Geological Survey observation wells (Fig. 5). The historical groundwater head data were used to derive a groundwater head distribution for January 1, 1975 as the initial condition for the groundwater model. The historical groundwater head data were also used to derive groundwater head values at the model boundaries as the time-varied specified head boundary condition for the groundwater model. The monthly stress period and monthly time step were adopted owing to available monthly pumpage records (1975–2014) for the study area; therefore, there are 480 stress periods. Surficial recharge in the model domain was neglected due to a confining unit on the top of the MRAA and the “400-foot” sand.

The MODFLOW well package (MNW2; Konikow et al. 2009) was used to model pumping wells screened in a single sand or multiple sands. The time-variant specified head

(CHD) package was used for the boundary condition, which is assigned to all boundary active cells. The Baton Rouge fault and the Denham Springs-Scotlandville fault are considered as horizontal flow barriers and their permeability is characterized by the hydraulic characteristic (HC; Hsieh and Freckleton 1993). The two faults were simulated using the horizontal flow barrier (HFB) package. The PCGN solver (Naff and Banta 2008) was used. The model parameters to be estimated are hydraulic conductivity, specific storage, and fault hydraulic characteristic.

Model calibration results and estimated model parameters

The parallel CMA-ES (Elshall et al. 2015) was implemented to minimize the root mean square error (RMSE) between the calculated and observed groundwater heads. Parallel computation was carried using a supercomputer at Louisiana State

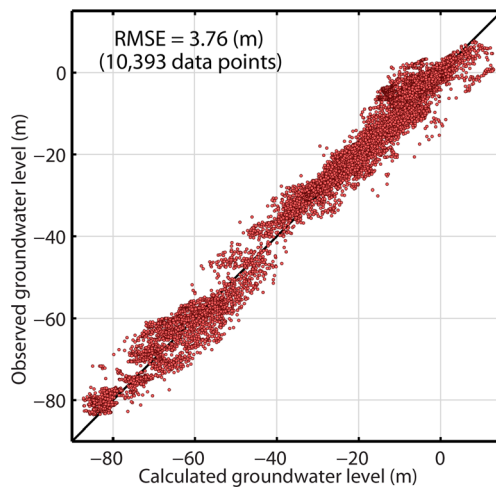


Fig. 9 Scatter plot for observed groundwater level vs. calculated groundwater level

University, which has 382 compute nodes. Each compute node is equipped with two 10-core 2.8GHz Intel Ivy Bridge-EP processors. Hansen and Ostermeier (2001) and Hansen et al. (2003) recommended a good population size for CMA-ES to be tenfold of unknown variables. Since the number of model parameters to be estimated is 38, the study used a population size of 380. To maximize the efficiency of parallel computing, the number of processors is equal to the population size; therefore, 19 compute nodes were used to conduct model calibration using the parallel CMA-ES.

Given that the algorithm parallelization time is less than 1 s per iteration, the speedup of the parallel CMA-ES is roughly equal to population size. Running the Baton Rouge groundwater model takes about 18 h and using 380 processors for model calibration takes 75 days with 100 iterations. It would need 78 years without parallel computing. The parallel CMA-ES significantly reduced calibration time.

The groundwater model was calibrated using 10,393 transient groundwater heads from 42 US Geological Survey

observation wells (Fig. 5) from January 1, 1975 to December 31, 2014. Model calibration found a good match between observed and calculated groundwater heads shown in Fig. 9. The RMSE is 3.76 m. The estimated parameter values of hydraulic conductivity, specific storage and fault hydraulic characteristic are given in Table 1. The calibration result indicates that the Holocene aquifer (MRAA) to the Pliocene aquifer (“1,700-foot” sand) have relatively lower hydraulic conductivity than that of Miocene aquifers (“2,000-foot” sand to “2,800-foot” sand). Specific storage is between 10^{-4} and 10^{-5} m^{-1} for all sands. Hydraulic characteristic for the faults varies across seven orders of magnitude. The calibration result indicates very low permeability for the Denham Springs-Scotlandville fault at the “2,000-foot” sand, which implies very limited freshwater flow across the fault. The calibration result also indicates very low hydraulic characteristic for the Baton Rouge fault at the “600-foot” sand, which limits groundwater flowing from south of the fault. In general, the calibration result supports the previous study (Elshall et al. 2015) that the Baton Rouge fault and the Denham Springs-Scotlandville fault are low-permeability leaky faults that restrict horizontal flow.

Groundwater flow simulation and budget analyses

Simulated groundwater levels in December 31, 2014 are presented in Fig. 10 using the estimated parameters in Table 1. The low groundwater level in the aquifers between the faults is caused by the heavy pumping. Groundwater levels decrease in depth indicating more groundwater withdrawal from deep sands. The “2,000-foot” sand has the lowest groundwater level due to heavy pumping in the Industrial District. The downward head difference between the shallow sands and the deep sands warrants the purpose of the connector well EB-1293 (Fig. 8) that connects the “800-foot” sand and the “1,500-foot” sand in order to raise groundwater level in the “1,500-foot” sand (Dial and Cardwell 1999).

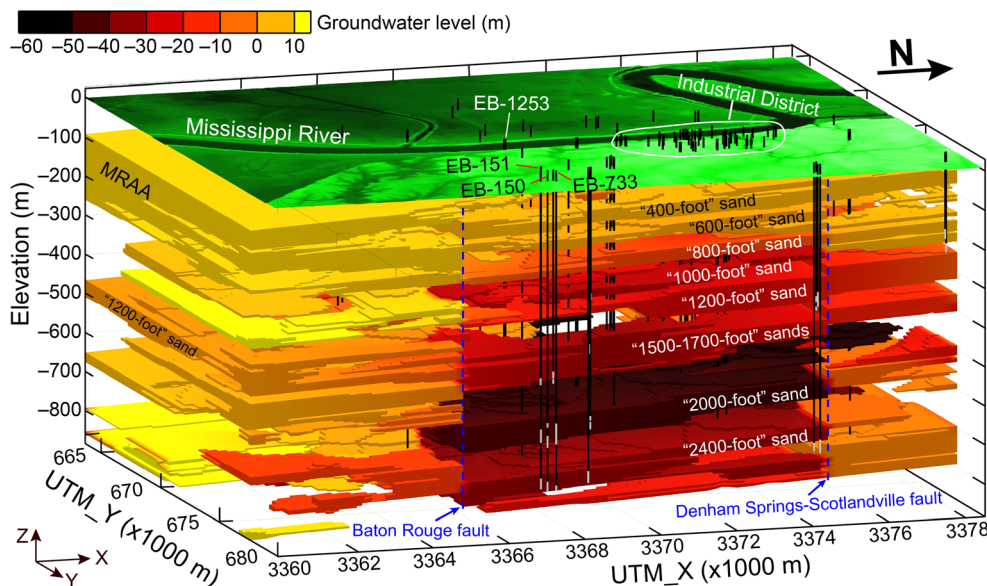
Table 1 Estimated model parameters for the Baton Rouge aquifer system. K hydraulic conductivity, S_s specific storage, DSS Denham Springs-Scotlandville, BR Baton Rouge; HC hydraulic characteristic

Series ^a	Aquifer	K (m/day)	S_s (1/m)	HC of DSS Fault (1/day)	HC of BR Fault (1/day)
Holocene	MRAA	25.0 ^b	1.96E-05	5.99E-03	8.99E-05
Pleistocene	“400-foot” sand	25.0 ^b	1.96E-05	5.99E-03	8.99E-05
	“600-foot” sand	5.0	6.24E-05	9.00E-02 ^b	3.00E-07 ^b
	“800-foot” sand	21.5	3.13E-05	4.45E-03	5.26E-03
Pliocene	“1000-foot” sand	35.6	3.42E-05	4.28E-01	8.69E-03
	“1200-foot” sand	15.6	3.80E-05	9.00E-02 ^b	2.68E-03
	“1500-foot” sand	22.2	3.79E-05	1.53E-02	2.40E-03
	“1700-foot” sand	22.2	8.32E-05	1.15E-01	1.97E-03
	“2000-foot” sand	100.0	2.81E-05	1.00E-06 ^b	4.47E-03
Miocene	“2400-foot” sand	55.0	9.00E-05 ^b	8.48E-04	9.11E-04
	“2800-foot” sand	60.0	5.68E-05	—	—

^a Source: Tomaszewski (1996)

^b Bound value

Fig. 10 Simulated groundwater level in December 31, 2014 in 11 aquifers. Vertical lines are pumping wells. EB-150, EB-151, EB-733, and EB-1253 are screened in both the “2,000-foot” sand and the “2,400-foot” sand



Moreover, Fig. 10 indicates potential flow from the “2,400-foot” sand to the “2,000-foot” sand due to upward head difference. The simulation result indicates that the “2,400-foot” sand may recharge the “2,000-foot” sand through four pumping wells (EB-150, EB-151, EB-733, and EB-1253) (Fig. 10), which were screened in both sands, when pumps are not running.

The distinct head differences across the faults shown in Fig. 10 are due to low permeability of the faults that restrict

horizontal flow. Nevertheless, regarding the concern of salt-water intrusion (Morgan and Winner 1964; Whiteman 1979; Tomaszewski 1996; Lovelace 2007), the modeling result indicates the Baton Rouge fault to be a leaky fault that permits a certain amount of salty groundwater flow northward through the fault.

Analyses of 1975–2014 water budget shown in Fig. 11a–d estimate about 580,000 m³/day of groundwater flow annually

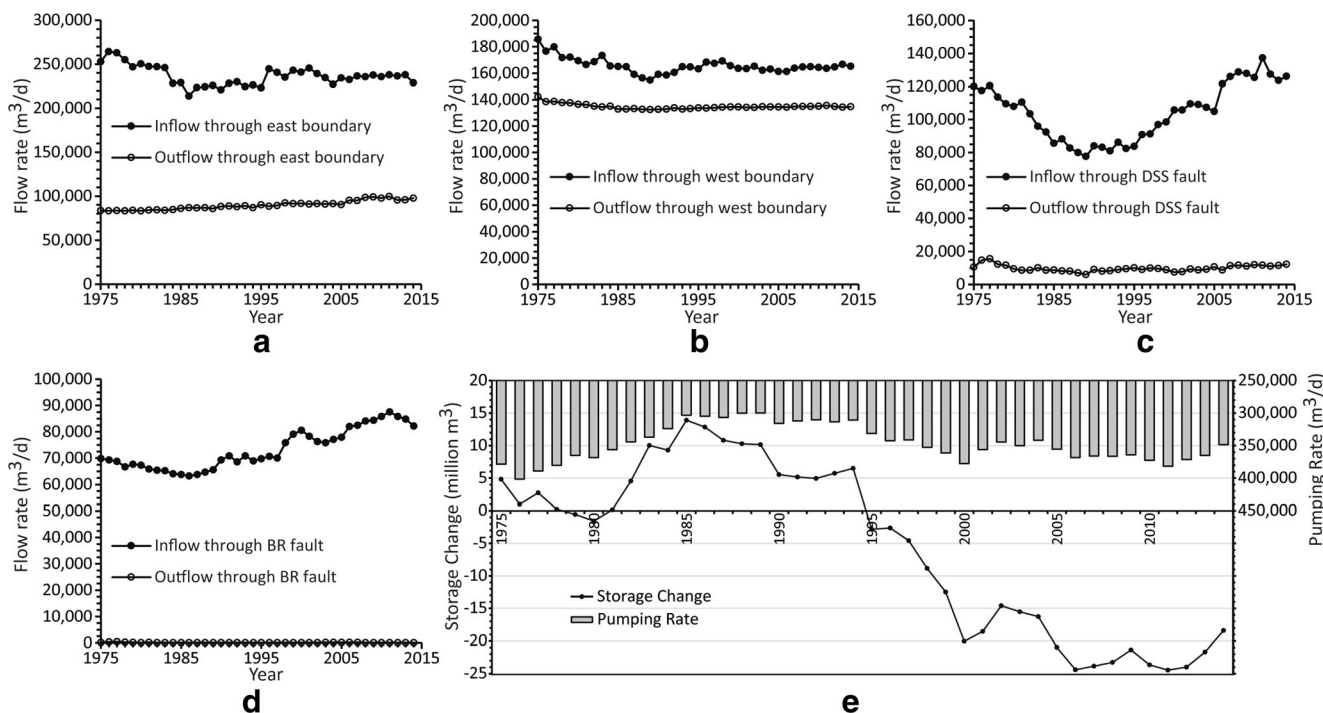
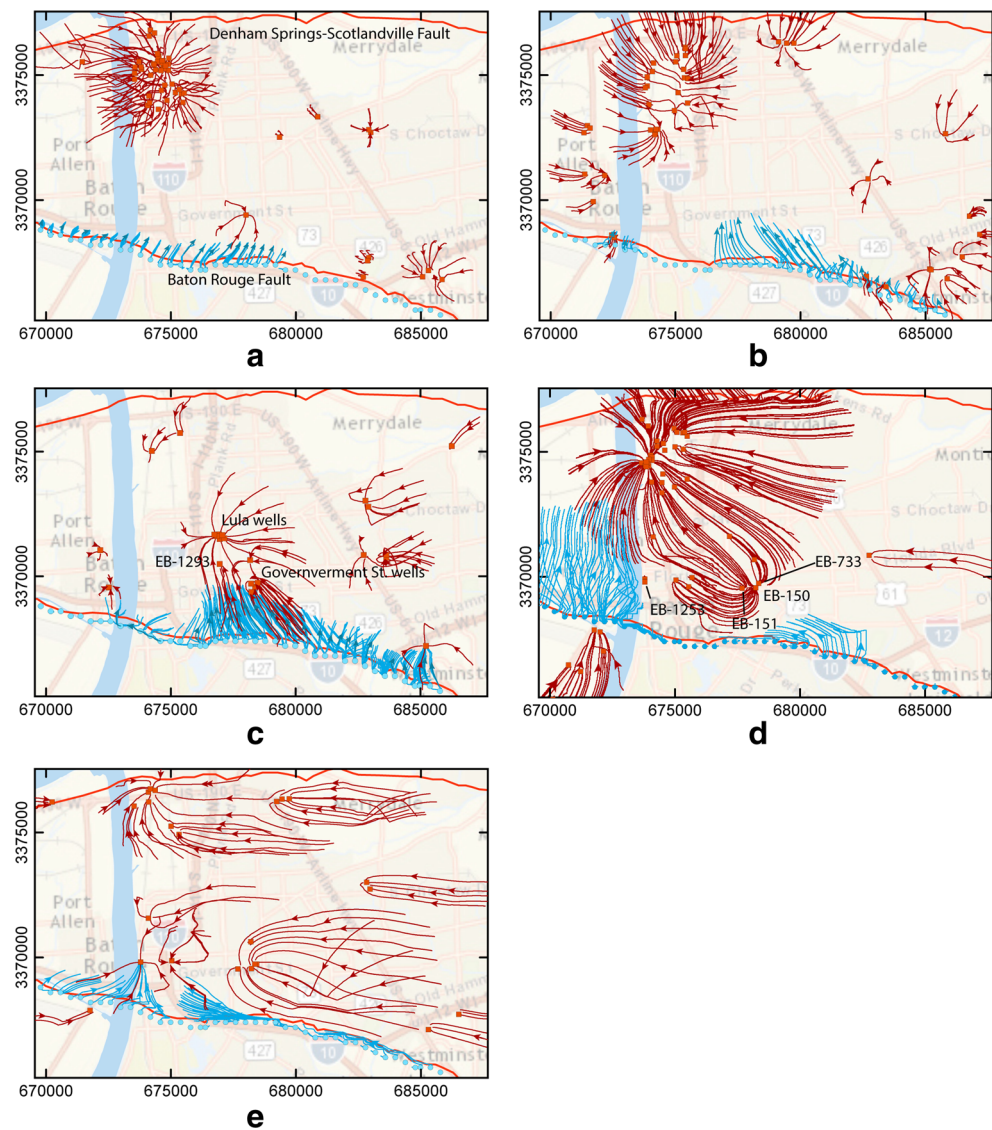


Fig. 11 Simulated groundwater budget for the aquifers between the Baton Rouge fault and the Denham Springs-Scotlandville fault. Inflow and outflow (m³/day) through a east boundary of model domain, b west boundary of model domain, c Denham Springs-Scotlandville (DSS) fault,

and d Baton Rouge (BR) fault. e Annual pumping rate (m³/day) and annual groundwater storage change (million m³) with respect to the beginning groundwater storage of 1975

Fig. 12 Particle tracking simulation from January 1, 1975 to December 31, 2014 for **a** MRAA “400–600–800-foot” sands, **b** “1,000–1,200-foot” sands, **c** “1,500–1,700-foot” sands, **d** “2,000-foot” sand, and **e** “2,400-foot” sand. *Squares* are pumping and injection wells. *Red lines* and *blue lines* represent backward tracking and forward tracking of particle traces, respectively



into the aquifers between the two faults. About 70% of the total inflow comes from the east and west boundaries of the model domain, about 17% of the total inflow comes through the Denham Springs-Scotlandville fault, and about 13% of the total inflow comes through the Baton Rouge fault. About 581,300 m³/day of annual groundwater outflow is estimated, which is greater than the annual total inflow. The majority of the total outflow is groundwater pumping, accounting for about 59% of the total outflow. Groundwater outflow through the east and west boundaries of the model domain is estimated at about 39% of the total outflow. Groundwater outflow through the faults is very limited. In average, about 100 m³/day of groundwater annually flows southward through the Baton Rouge fault, and about 9,800 m³/day of groundwater annually flows northward through the Denham Springs-Scotlandville fault.

Figure 11e shows the estimated annual storage change with respect to the beginning storage of 1975. The storage

change is strongly corresponding to groundwater pumping. Groundwater storage was generally increased before 1995 due to groundwater pumping decrease. Groundwater storage started to fall below the beginning storage of 1975 in response to groundwater pumping increase. The study estimates about 18.4 million m³ of groundwater storage loss in 2014.

Particle tracking

MODPATH (Pollock 2012) was used to track groundwater flow towards pumping wells and through the Baton Rouge fault. Four imaginary particles were placed at each pumping well and at each cell immediately south of the Baton Rouge fault. By using forward tracking and backward tracking, Fig. 12 shows the horizontal-plane projections of 40-year 3D flow paths from January 1, 1975 to December 31, 2014. The longer paths in the “2,000-foot” sand and the “2,400-

foot” sand owing to heavy pumping and high hydraulic conductivity. The long outward flow paths from the pumping wells EB-150, EB-151, and EB-733 in Fig. 12d indicate strong recharge from the “2,400-foot” sand to the “2,000-foot” sand. While the model did show recharge from the “2,400-foot” sand to the “2,000-foot” sand in pumping well EB-1253, the outward flow path from EB-1253 is shortened by the strong pumping of its nearby wells. The flow paths across the Baton Rouge fault indicate fault leaky areas. The simulation result shows the possibility that groundwater south of the Baton Rouge fault can reach some pumping wells near the fault within 40 years.

Conclusions

This study presents a general framework to develop groundwater models for fluvial-in-origin aquifer systems with a focus on grid generation and model calibration, which are two crucial modeling steps. The developed grid generation technique can handle a large number of well logs and preserve facies geometries of complex hydrostratigraphic architecture by using fine vertical discretization. This includes coalescences, pinch-outs, and narrow hydraulic connections through faults. It improves the shortcomings of the solid method and the pre-defined grid method and reduces model structure error for groundwater models.

The model development framework is successfully applied to the Baton Rouge aquifer system. The well log information and the constructed hydrostratigraphy confirm the complexity of the fluvial-in-origin aquifer system. Potential leaky areas in the geological faults are identified. To meet the current structural complexity, a large number of model layers is needed in order to model the 11 aquifers underneath Baton Rouge. The developed groundwater model is very time-consuming. Using parallel computing is necessary for automatic model calibration.

The calibration result indicates Miocene aquifers have higher hydraulic conductivity than Pliocene-Holocene aquifers. The Baton Rouge fault and the Denham Springs-Scotlandville fault are identified as low-permeability leaky faults. The estimated hydraulic characteristic of the faults varies over seven orders of magnitude. Specifically, the calibration result indicates very limit freshwater flow across the Denham Springs-Scotlandville fault for the “2,000-foot” sand and very limit freshwater flow across the Baton Rouge fault for the “600-foot” sand.

The model result indicates groundwater level decreasing with depth. The “2,000-foot” sand shows the lowest groundwater level owing to heavy industrial pumping. Potential groundwater flow from the “2,400-foot” sand to the “2,000-foot” sand is indicated by the upward head gradient between these two sands.

The water budget analyses for the sands between the geological faults indicate that 70% of the total inflow comes from the east and west boundaries of the model domain and about 30% of total inflow comes through the two faults. It is estimated that 13% of the total inflow comes from the Baton Rouge fault. Groundwater pumping is estimated about 59% of total outflow. The water budget analyses also indicate that groundwater storage is significantly depleted since 1995 due to excessive groundwater pumping. The particle tracking analysis reveals the location of the leaky areas of the Baton Rouge fault. The result also indicates that the groundwater south of the Baton Rouge fault can reach some pumping wells near the fault within 40 years.

The developed grid generation technique is highly flexible to include new well logs and to re-generate structured MODFLOW grids. Future additions in this study may include new wireline well logs and good-quality driller’s logs to update the constructed hydrostratigraphy. Including more geological and geophysical data may lead to a more complex groundwater model. A future study may develop a grid generation technique for unstructured MODFLOW grids (MODFLOW-USG) to handle complex hydrostratigraphy and reduce MODFLOW computation time.

Acknowledgements The study was supported in part by the LSU Economic Development Assistantship (EDA) to H. Pham, the US Geological Survey through Louisiana Water Resources Research Institute (G16AP00056), Louisiana Board of Regents and CAGWCC (LEQSF(2015–18)-RD-B-03). The authors thank the US Geological Survey, the Louisiana Department of Natural Resources, and the Capital Area Groundwater Conservation Commission for providing pertinent data to construct the groundwater model. LSU High Performance Computing and LSU Center for Computation and Technology are acknowledged for providing a supercomputer, SuperMIC for this study. AE Michael Sukop and two anonymous reviewers are greatly appreciated for their constructive comments. Readers who are interested in the grid generation code may contact Frank Tsai.

References

- Abbaspour KC, Schulin R, van Genuchten MT (2001) Estimating unsaturated soil hydraulic parameters using ant colony optimization. *Adv Water Resour* 24:827–841. doi:10.1016/S0309-1708(01)00018-5
- Alabert K, Modot V (1993) Stochastic models of reservoir heterogeneity: Impact on connectivity and average permeabilities. In: SEG Technical Program Expanded Abstracts 1993. Society of Exploration Geophysicists, Tulsa, OK, pp 340–340
- Anderson CE, Hanor JS, Tsai FT-C (2013) Sources of salinization of the Baton Rouge Aquifer System, southeastern Louisiana. *Gulf Coast Assoc Geol Soc Trans* 2013:3–12
- Bassiouni Z (1994) Theory, measurement, and interpretation of well logs. Henry L. Doherty Memorial Fund of AIME, Society of Petroleum Engineers, Richardson, TX
- Bense VF, Person MA (2006) Faults as conduit-barrier systems to fluid flow in siliciclastic sedimentary aquifers. *Water Resour Res* 42, W05421. doi:10.1029/2005WR004480

- Berg SJ, Illman WA (2015) Comparison of hydraulic tomography with traditional methods at a highly heterogeneous site. *Groundwater* 53: 71–89. doi:10.1111/gwat.12159
- Bianchi M, Zheng C, Wilson C et al (2011) Spatial connectivity in a highly heterogeneous aquifer: from cores to preferential flow paths. *Water Resour Res* 47, W05524. doi:10.1029/2009WR008966
- Bowling JC, Rodriguez AB, Harry DL, Zheng C (2005) Delineating alluvial aquifer heterogeneity using resistivity and GPR data. *Ground Water* 43:890–903. doi:10.1111/j.1745-6584.2005.00103.x
- Carle SF (1999) T-PROGS: transition probability geostatistical software. University of California, Davis, CA
- Carle SF, Fogg GE (1996) Transition probability-based indicator geostatistics. *Math Geol* 28:453–476. doi:10.1007/BF02083656
- Chamberlain EL, Hanor JS, Tsai FT-C (2013) Sequence stratigraphic characterization of the Baton Rouge aquifer system, southeastern Louisiana. *Gulf Coast Assoc Geol Soc Trans* 63:125–136
- Cooley RL (1985) A comparison of several methods of solving nonlinear regression groundwater flow problems. *Water Resour Res* 21:1525–1538. doi:10.1029/WR021i010p01525
- de Marsily G, Delay F, Gonçalves J et al (2005) Dealing with spatial heterogeneity. *Hydrogeol J* 13:161–183. doi:10.1007/s10040-004-0432-3
- dell’Arciprete D, Bersezio R, Felletti F et al (2012) Comparison of three geostatistical methods for hydrofacies simulation: a test on alluvial sediments. *Hydrogeol J* 20:299–311. doi:10.1007/s10040-011-0808-0
- Deutsch CV, Journel AG (1997) *GSLIB: Geostatistical Software Library and user’s guide*, 2nd edn. Oxford University Press, New York
- Dial DC, Cardwell GT (1999) A connector well to protect water-supply wells in the “1,500-ft” sand of the Baton Rouge, Louisiana area from saltwater encroachment: Capital Area Ground Water Conservation Commission Bulletin no. 5, 17p
- Doherty J (2015) Calibration and uncertainty analysis for complex environmental models. Watermark, Brisbane, Australia
- Doherty J, Brebber L, Whyte P (1994) PEST: Model-independent parameter estimation. <http://www.pesthomepage.org/>. Accessed January 2017
- El Harrouni K, Ouazar D, Walters GA, Cheng AH-D (1996) Groundwater optimization and parameter estimation by genetic algorithm and dual reciprocity boundary element method. *Eng Anal Bound Elem* 18:287–296. doi:10.1016/S0955-7997(96)00037-9
- Elshall AS, Tsai FT-C, Hanor JS (2013) Indicator geostatistics for reconstructing Baton Rouge aquifer–fault hydrostratigraphy, Louisiana, USA. *Hydrogeol J* 21:1731–1747. doi:10.1007/s10040-013-1037-5
- Elshall AS, Pham HV, Tsai FT-C et al (2015) Parallel inverse modeling and uncertainty quantification for computationally demanding groundwater-flow models using covariance matrix adaptation. *J Hydrol Eng* 20:4014087. doi:10.1061/(ASCE)HE.1943-5584.0001126
- Fienen MN, Muffels CT, Hunt RJ (2009) On constraining pilot point calibration with regularization in PEST. *Ground Water* 47:835–844. doi:10.1111/j.1745-6584.2009.00579.x
- Galloway WE (1977) *Catahoula Formation of the Texas Coastal Plain: depositional systems, composition, structural development, groundwater flow history, and uranium distribution*. Bureau of Economic Geology, Texas Univ., Austin, TX
- Gill MK, Kaheil YH, Khalil A et al (2006) Multiobjective particle swarm optimization for parameter estimation in hydrology. *Water Resour Res* 42, W07417. doi:10.1029/2005WR004528
- Gómez-Hernández JJ, Wen X-H (1998) To be or not to be multi-Gaussian? A reflection on stochastic hydrogeology. *Adv Water Resour* 21:47–61. doi:10.1016/S0309-1708(96)00031-0
- Griffith JM (2003) *Hydrogeologic framework of southeastern Louisiana*. Louisiana Department of Transportation and Development, Baton Rouge, LA
- Hansen N, Ostermeier A (2001) Completely derandomized self-adaptation in evolution strategies. *Evol Comput* 9:159–195. doi:10.1162/106365601750190398
- Hansen N, Müller SD, Koumoutsakos P (2003) Reducing the time complexity of the derandomized evolution strategy with covariance matrix adaptation (CMA-ES). *Evol Comput* 11:1–18
- Harbaugh AW (2005) MODFLOW-2005, The U.S. Geological Survey Modular Ground-Water Model: the ground-water flow process. In: Modeling techniques, book 6, section A, US Geological Survey, Reston, VA, 253 pp
- Hendricks Franssen HJ, Alcolea A, Riva M et al (2009) A comparison of seven methods for the inverse modelling of groundwater flow: application to the characterisation of well catchments. *Adv Water Resour* 32:851–872. doi:10.1016/j.advwatres.2009.02.011
- Hilchie DW (1982) *Advanced well log interpretation*. Hilchie, Golden, CO
- Hill MC, Tiedeman CR (2007) *Effective groundwater model calibration: with analysis of data, sensitivities, predictions, and uncertainty*, 1st edn. Wiley, Chichester, UK
- Hsieh PA, Freckleton JR (1993) Documentation of a computer program to simulate horizontal-flow barriers using the U.S. Geological Survey’s Modular three-dimensional finite-difference ground-water flow model. US Geological Survey, Reston, VA
- Hu LY, Chugunova T (2008) Multiple-point geostatistics for modeling subsurface heterogeneity: a comprehensive review. *Water Resour Res* 44, W11413. doi:10.1029/2008WR006993
- Hunt RJ, Doherty J, Tonkin MJ (2007) Are models too simple? Arguments for increased parameterization. *Ground Water* 45:254–262. doi:10.1111/j.1745-6584.2007.00316.x
- Johnson NM (1995) Characterization of alluvial hydrostratigraphy with indicator semivariograms. *Water Resour Res* 31:3217–3227. doi:10.1029/95WR02571
- Johnson NM, Dreiss SJ (1989) Hydrostratigraphic interpretation using indicator geostatistics. *Water Resour Res* 25:2501–2510. doi:10.1029/WR025i012p02501
- Jones NL, Budge TJ, Lemon AM, Zundel AK (2002) Generating MODFLOW grids from boundary representation solid models. *Ground Water* 40:194–200. doi:10.1111/j.1745-6584.2002.tb02504.x
- Journel AG (1983) Nonparametric estimation of spatial distributions. *J Int Assoc Math Geol* 15:445–468. doi:10.1007/BF01031292
- Journel AG (2005) Beyond covariance: the advent of multiple-point geostatistics. In: Leuangthong O, Deutsch CV (eds) *Geostatistics Banff 2004*. Springer, Dordrecht, The Netherlands, pp 225–233. doi:10.1007/978-1-4020-3610-1_23
- Karpouzos DK, Delay F, Katsifarakis KL, de Marsily G (2001) A multipopulation genetic algorithm to solve the inverse problem in hydrogeology. *Water Resour Res* 37:2291–2302. doi:10.1029/2000WR900411
- Kerr DR, Jirik LA (1990) Fluvial architecture and reservoir compartmentalization in the Oligocene Middle Frio formation, south Texas. *Gulf Coast Assoc Geol Soc Trans* 40:373–380
- Koch J, He X, Jensen KH, Refsgaard JC (2014) Challenges in conditioning a stochastic geological model of a heterogeneous glacial aquifer to a comprehensive soft data set. *Hydrol Earth Syst Sci* 18:2907–2923. doi:10.5194/hess-18-2907-2014
- Koltermann CE, Gorelick SM (1996) Heterogeneity in sedimentary deposits: a review of structure-imitating, process-imitating, and descriptive approaches. *Water Resour Res* 32:2617–2658. doi:10.1029/96WR00025
- Konikow LF, Homberger GZ, Halford KJ, Hanson RT (2009) Revised multi-node well (MNW2) package for MODFLOW ground-water flow model. US Geol Surv Techniques Methods 6-A30, 67 pp
- Krauß T, Cullmann J (2012) Towards a more representative parametrisation of hydrologic models via synthesizing the strengths

- of particle swarm optimisation and robust parameter estimation. *Hydrol Earth Syst Sci* 16:603–629. doi:10.5194/hess-16-603-2012
- Lee S-Y, Carle SF, Fogg GE (2007) Geologic heterogeneity and a comparison of two geostatistical models: sequential Gaussian and transition probability-based geostatistical simulation. *Adv Water Resour* 30:1914–1932. doi:10.1016/j.advwatres.2007.03.005
- Lemon AM, Jones NL (2003) Building solid models from boreholes and user-defined cross-sections. *Comput Geosci* 29:547–555. doi:10.1016/S0098-3004(03)00051-7
- Lovelace JK (2007) Chloride concentrations in ground water in East and West Baton Rouge parishes, Louisiana, 2004–05. US Geological Survey, Reston, VA
- McCulloh RP, Heinrich PV (2013) Surface faults of the south Louisiana growth-fault province. *Geol Soc Am Spec Pap* 493:37–49. doi:10.1130/2012.2493(03)
- Meyer RR, Turcan AN (1955) *Geology and Ground-Water Resources of the Baton Rouge Area, Louisiana*. US Government Printing Office, Washington: Geological Survey Water-Supply Paper 1296, 144p
- Miall AD (2010) Alluvial deposits. In: James NP, Dalrymple RW (eds) *Facies models 4*, 4th edn. Geological Association of Canada, St. John's, NL
- Morgan CO, Winner MD (1964) Salt-water encroachment in aquifers of the Baton Rouge area: preliminary report and proposal. Louisiana Department of Public Works, Baton Rouge, LA
- Naff RL, Banta ER (2008) The U.S. Geological Survey modular groundwater model: PCGN—a preconditioned conjugate gradient solver with improved nonlinear control. *US Geol Surv Open-File Rep* 2008-1331
- Olea RA (1999) *Geostatistics for engineers and Earth scientists*, 1999th edn. Springer, Boston
- Panday S, Langevin C, Niswonger R et al (2013) MODFLOW–USG version 1: an unstructured grid version of MODFLOW for simulating groundwater flow and tightly coupled processes using a control volume finite-difference formulation. *US Geological Survey Techniques and Methods*, book 6, chap A45, US Geological Survey, Reston, VA, 66 pp
- Poeter EP, Hill MC (1999) UCODE, a computer code for universal inverse modeling. *Comput Geosci* 25:457–462
- Pollock DW (2012) User guide for MODPATH version 6: a particle tracking model for MODFLOW. US Geological Survey, Reston, VA
- Proce CJ, Ritzi RW, Dominic DF, Dai Z (2004) Modeling multiscale heterogeneity and aquifer interconnectivity. *Ground Water* 42:658–670. doi:10.1111/j.1745-6584.2004.tb02720.x
- Schlumberger (1972) *Log interpretation, vol 1: principles*. Schlumberger, New York
- Strebelle S (2002) Conditional simulation of complex geological structures using multiple-point statistics. *Math Geol* 34:1–21. doi:10.1023/A:1014009426274
- Sun N-Z (1994) *Inverse problems in groundwater modeling*, 1994th edn. Springer, Heidelberg, Germany
- Tomaszewski DJ (1996) Distribution and movement of saltwater in aquifers in the Baton Rouge area, Louisiana, 1990–92. Louisiana Department of Transportation and Development, Baton Rouge, LA
- Vrugt JA, Gupta HV, Bouten W, Sorooshian S (2003) A shuffled complex evolution metropolis algorithm for optimization and uncertainty assessment of hydrologic model parameters. *Water Resour Res* 39:1201. doi:10.1029/2002WR001642
- Vrugt JA, Stauffer PH, Wöhling T et al (2008) Inverse modeling of subsurface flow and transport properties: a review with new developments. *Vadose Zone J* 7:843–864. doi:10.2136/vzj2007.0078
- Wang QJ (1997) Using genetic algorithms to optimise model parameters. *Environ Model Softw* 12:27–34. doi:10.1016/S1364-8152(96)00030-8
- Western AW, Blöschl G, Grayson RB (2001) Toward capturing hydrologically significant connectivity in spatial patterns. *Water Resour Res* 37:83–97. doi:10.1029/2000WR900241
- Whiteman CD (1979) Saltwater Encroachment in the 600-foot and 1,500-foot sands of the Baton Rouge area, Louisiana, 1966–78, including a discussion of saltwater in other sands. Office of Public Works Water Resources technical report no. 19, Louisiana Department of Transportation and Development, Baton Rouge, LA
- Whiteman CD (1980) Measuring local subsidence with extensometers in the Baton Rouge area, Louisiana, 1975–79. Office of Public Works Water Resources technical report no. 20, Louisiana Department of Transportation and Development, Baton Rouge, LA, 18 pp
- Yeh WW-G (2015) Review: Optimization methods for groundwater modeling and management. *Hydrogeol J* 23:1051–1065. doi:10.1007/s10040-015-1260-3
- Zhang H, Harter T, Sivakumar B (2006) Nonpoint source solute transport normal to aquifer bedding in heterogeneous, Markov chain random fields. *Water Resour Res* 42, W06403. doi:10.1029/2004WR003808
- Zheng C, Wang P (1996) Parameter structure identification using tabu search and simulated annealing. *Adv Water Resour* 19:215–224. doi:10.1016/0309-1708(96)00047-4
- Zheng C, Wang PP (2003) MGO: a modular groundwater optimizer incorporating modflow/mt3dms, documentation and user's guide. Groundwater Systems Research, Tuscaloosa, AL
- Zinn B, Harvey CF (2003) When good statistical models of aquifer heterogeneity go bad: a comparison of flow, dispersion, and mass transfer in connected and multivariate Gaussian hydraulic conductivity fields. *Water Resour Res* 39:1051. doi:10.1029/2001WR001146